Plant-derived angiogenin fusion protein's cytoprotective effect on trabecular meshwork damage induced by Benzalkonium chloride in mice

Jae Hoon Jeong [1, 2, 3], **Soo Jin Lee** [4], **Kisung Ko** [5], **Jeong Hwan Lee** [5], **Jungmook Lyu** [3, 6], **Moon Hyang Park** [7], **Jaeku Kang** [2, 8], **Jae Chan Kim** [Corresp. 4]

[1] Departement of Ophthalmology, Konyang University Hospital, Daejeon, South Korea

[2] Myunggok Medical Research Institute, Konyang University, Daejeon, South Korea

[3] Myunggok Eye Research Institute, Konyang University, Daejeon, South Korea

[4] Departement of Ophthalmology, Chung-Ang University Hospital, Seoul, South Korea

[5] Therapeutic Protein Engineering Lab / College of Medicine, Chung-Ang University, Seoul, South Korea

[6] Department of Medical Science, Konyang University, Daejeon, South Korea

[7] Department of Pathology, Konyang University Hospital, Daejeon, South Korea

[8] Department of Pharmacology / College of Medicine, Konyang University, Daejeon, South Korea

Corresponding Author: Jae Chan Kim
Email address: jck50ey@daum.net

Background: Benzalkonium chloride (BAK), commonly used in glaucoma treatment, is an eye drop preservative with dose-dependent toxicity. Previous studies have observed the multi-functional benefits of angiogenin (ANG) against glaucoma. In our study, we evaluated ANG's cytoprotective effect on the trabecular meshwork (TM) damage induced by BAK. Additionally, we developed a plant-derived ANG fusion protein and evaluated its effect on TM structure and function.

Methods: We synthesized plant-derived ANG (ANG-FcK) by fusing immunoglobulin G's Fc region and KDEL to conventional recombinant human ANG (Rh-ANG) purified from transgenic tobacco plants. We established a mouse model using BAK to look for degenerative changes in the TM, and to evaluate the protective effects of ANG-FcK and Rh-ANG. Intraocular pressure (IOP) was measured for 4 weeks and ultrastructural changes, deposition of fluorescent microbeads, type I and IV collagen, fibronectin, laminin, and α-SMA expression were analyzed after the mice were euthanized.

Results: TM structural and functional degeneration were induced by 0.1% BAK instillation in mice. ANG co-treatment preserved TM outflow function, which we measured using IOP and a microbead tracer. ANG prevented phenotypic and ultrastructure changes, and that protective effect might be related to the anti-fibrosis mechanism. We observed a similar cytoprotective effect in the BAK-induced degenerative TM mouse model, suggesting that plant-derived ANG-FcK could be a promising glaucoma treatment.

Plant-derived angiogenin fusion protein's cytoprotective effect on trabecular meshwork damage induced by Benzalkonium chloride in mice

Jae Hoon Jeong[1,2,3], Soo Jin Lee[4], Kisung Ko[5], Jeong Hwan Lee[5], Jungmook Lyu[3,6], Moon Hyang Park[7], Jaeku Kang[2,8], Jae Chan Kim[4]

[1]Departement of Ophthalmology, Konyang University Hospital, Daejeon, Republic of Korea
[2]Konyang University Myunggok Medical Research Institute, Daejeon, Republic of Korea
[3]Konyang University Myunggok Eye Research Institute, Daejeon, Republic of Korea
[4]Department of Ophthalmology, Chung-Ang University Hospital, Seoul, Republic of Korea
[5]Therapeutic Protein Engineering Lab, College of Medicine, Chung-Ang University, Seoul, Republic of Korea
[6]Department of Medical Science, Konyang University, Daejeon, Republic of Korea
[7]Department of Pathology, Konyang University Hospital, Daejeon, Republic of Korea
[8]Department of Pharmacology, College of Medicine, Konyang University, Daejeon, Republic of Korea

Corresponding Author
Jae Chan Kim, MD, PhD
Department of Ophthalmology, Chung-Ang University Hospital, Seoul, Republic of Korea
E-mail: jck50ey@daum.net

ABSTRACT

Background: Benzalkonium chloride (BAK), commonly used in glaucoma treatment, is an eye drop preservative with dose-dependent toxicity. Previous studies have observed the multi-functional benefits of angiogenin (ANG) against glaucoma. In our study, we evaluated ANG's cytoprotective effect on the trabecular meshwork (TM) damage induced by BAK. Additionally, we developed a plant-derived ANG fusion protein and evaluated its effect on TM structure and function.

Methods: We synthesized plant-derived ANG (ANG-FcK) by fusing immunoglobulin G's Fc region and KDEL to conventional recombinant human ANG (Rh-ANG) purified from transgenic tobacco plants. We established a mouse model using BAK to look for degenerative changes in the TM, and to evaluate the protective effects of ANG-FcK and Rh-ANG. Intraocular pressure (IOP) was measured for 4 weeks and ultrastructural changes, deposition of fluorescent microbeads, type Ⅰ and Ⅳ collagen, fibronectin, laminin, and α-SMA expression were analyzed after the mice were euthanized.

Results: TM structural and functional degeneration were induced by 0.1% BAK instillation in mice. ANG co-treatment preserved TM outflow function, which we measured using IOP and a microbead tracer. ANG prevented phenotypic and ultrastructure changes, and that protective effect might be related to the anti-fibrosis mechanism. We observed a similar cytoprotective effect in the BAK-induced degenerative TM mouse model, suggesting that plant-derived ANG-FcK could be a promising glaucoma treatment.

Introduction

Glaucoma is a progressive optic neuropathy associated with various risk factors, including increased intraocular pressure (IOP) (Van Buskirk & Cioffi, 1992). IOP-related aqueous humor dynamics are currently the only known controllable factors for disease progression prevention. IOP-lowering eye drops contain therapeutic agents and additives (Inoue, 2014) such as benzalkonium chloride (BAK), a common ophthalmic preservative agent. Preservatives used in topical eye drops may cause ocular surface disorders, including superficial punctate keratitis, corneal erosion, conjunctival allergy, conjunctival injection, and anterior chamber inflammation (Baudouin, 2008; Noecker & Miller, 2011; Rosin & Bell, 2013).

After repeated instillations, BAK penetrates healthy eyes and is detected in both ocular surface structures and deeper tissues, such as the trabecular meshwork (TM) and optic nerve (Brignole-Baudouin et al., 2012). Eye drop preservatives may cause long-term trabecular degeneration and increased outflow resistance (Baudouin et al., 2012; Chang et al., 2015). Chronic or repeated eye drop use can have dose-dependent toxic effects, and should be examined when managing glaucoma. Although there are currently many anti-glaucomatous drugs formulated without preservatives, BAK is still frequently used in medicated eyedrops. Therefore, investigating protective agents against BAK-induced TM damage may improve the treatment and prevention of glaucoma.

Angiogenin (ANG), also known as Ribonuclease 5, has various functions (Gao & Xu, 2008) and associations with cancer and neurological diseases via its roles in angiogenesis and apoptosis suppression (Li et al., 2012; Steidinger et al., 2011; Tello-Montoliu et al., 2006). ANG is highly concentrated in normal tear fluid that has pooled overnight and helps maintain corneal avascularity. It is suggesting that ANG plays a physiological role which is separate from its

78 angiogenic role under normal ocular surface conditions (Sack et al., 2005). In addition, it has
79 been reported that ANG could be a candidate survival booster for transformed human TM cell
80 lines (Kim et al., 2016). However, the complete effects of BAK at the TM ultrastructure level
81 and ANG's protective mechanism are unclear. Since the trabecular outflow pathway of mice is
82 structurally and functionally similar to that of primates (Overby et al., 2014), we examined the
83 protective effect of ANG against BAK in mice TM. Additionally, considering that recombinant
84 human ANG (Rh-ANG) is expensive and plants are beneficial as a heterologous expression
85 system for large scale recombinant protein production (Jamal et al., 2009), we developed a plant-
86 derived ANG fusion protein using molecular farming. The aim of our study was to evaluate
87 ANG's efficacy in protecting TM structure and function, and to introduce molecular farming
88 technology to the ophthalmology field.

Materials and Methods

BAK-induced TM degenerative mouse model

All mouse experiments were conducted in compliance with the Association for Research in Vision and Ophthalmology Statement for the Use of Animals in Ophthalmic and Vision Research. The Institutional Animal Care and Use Committee in College of Medicine, Konyang University reviewed and approved the study protocol (P-16-22-A-01). The following toxicity model was used: instillation of one drop of 0.01%, 0.02%, 0.1%, and 0.2% BAK (Sigma Aldrich, Fluka, Buchs, Switzerland), respectively, twice a day (at 8 am and 8 pm) for 1 month, and a subconjunctival injection of 10 μL of 0.1% BAK. The mice's contralateral eye served as sham-operated controls. Subconjunctival intramuscular injection of a tiletamine and zolazepam-mixed agent (2 mg/kg, Zoletil; Virbac, Fort Worth, TX, USA) and xylazine (6 mg/kg, Rompun; Bayer, Leverkusen, Germany) was performed under general anesthesia.

Following a previous study where six rats were used to model BAK-induced TM degeneration (Baudouin et al., 2012), we initially assigned five mice to each toxicity model. However, four to five mice were included in each group due to unexpected deaths during the follow-up period. They were all male C57BL/6J Jms SLC mice (7 weeks old; 21–24 g) purchased from SLC Laboratory (Hamamatsu, Shizuoka, Japan). The mice were housed in clear cages with 12-hour light/12-hour dark cycles at 30–70% humidity and 22–24°C. Before BAK administration, the mice were allowed to acclimatize for 1 week and were provided tap water and food ad libitum. Their IOP was measured at 6 pm daily using a rebound tonometer (Tono-lab, iCare, Vantaa, Finland) without sedation, and we recorded the average values of three consecutive measurements. After 16 weeks, the mice were euthanized, and their eyes were enucleated for

112 histological analyses. The experimental protocols are summarized in Fig S1.

113

114 **Plant-derived ANG-FcK protein development**

115 We cloned cDNA fragments encoding the human ANG fused Fc region of immunoglobulin G-
116 tagged endoplasmic reticulum retention signal, KDEL (ANG-FcK), into a pBI121 plant
117 expression vector. The gene was then inserted with the alfalfa mosaic virus untranslated leader
118 sequence (AMV) from RNA4 under the control of the cauliflower mosaic virus 35S promoter
119 into the vector. We transferred the ANG-FcK gene expression cassette as a HindIII-EcoRI
120 fragment into the plant binary vector pBI121, and conducted Agrobacterium-mediated plant
121 transformation using the vector to generate transgenic tobacco (*Nicotiana tabacum*) lines
122 expressing ANG-FcK.

123 We homogenized 100 mg of transgenic plant leaf tissue in 300 μL of 1× PBS, resolved the
124 plant extracts by 12.5% sodium dodecyl sulfate polyacrylamide gel electrophoresis (SDS-
125 PAGE), and transferred them to a nitrocellulose membrane (Millipore, Bedford, MA, USA). The
126 membrane was incubated in blocking solution [5% (w/v) skim milk (Fluka) in 1× TBS, 0.05%
127 (v/v) Tween 20 (TBST)], followed by a primary anti-ANG antibody (1:250, Abcam Inc.,
128 Cambridge, MA, USA), and an anti-mouse IgG2a Fc fragment (1:3000, Jackson
129 ImmunoResearch Labs, West Grove, PA) conjugated to horseradish peroxidase was used as the
130 secondary antibody to detect ANG-FcK. The anti-ANG antibody we used for immunoblotting
131 recognized the full length ANG protein (Cat.# ab10600, Abcam Inc., Cambridge, MA, USA).
132 We used SuperSignal chemiluminescence substrate (Pierce, Rockford, IL, USA) to detect the
133 signal. Rh-ANG (R&D Systems, Minneapolis, MN, USA) was used as a positive control.

134 We used the same method of purifying plant-derived ANG-FcK as in our previous paper (Lim

et al., 2014). To purify plant-derived ANG-FcK, tobacco leaves were mixed with cold extraction buffer (37.5 mM Tris–HCl pH 7.5, 50 mM NaCl, 15 mM EDTA, 75 mM sodium citrate, and 0.2% sodium thiosulfate) and were homogenized in a HR2094 blender (Philips, Seoul, Korea). After homogenization, the leaves were centrifuged for 30 minutes at 8800 × g at 4 ℃, the supernatant was filtered using Miracloth (Merck, Darmstadt, Germany), and extra pure acetic acid was added to adjust the pH to 5.1. We centrifuged the solution at 10200 × *g* for 30 min at 4°C, brought up the pH to 7.0 by adding 3 M Tris–HCl, and added ammonium sulfate to a saturation of 8%. After centrifugation at 8800 × *g* for 30 min at 4°C, we discarded the precipitate and added ammonium sulfate to the supernatant to 40% saturation. After overnight incubation at 4°C, the solution was centrifuged, the pellet was resuspended in extraction buffer to 1/10 of the original volume, and the final solution was centrifuged at 10200 × *g* for 30 min at 4°C. The supernatant was filtered through a 0.45-mm filter and loaded onto a HiTrap Protein A column (Pharmacia, Uppsala, Sweden). We applied soluble protein extract to a protein A column (GE Healthcare, Piscataway, NJ, USA) and dialyzed elutes of plant-derived ANG-FcK protein against 1× PBS buffer. Aliquots were frozen in liquid nitrogen and stored at -80°C for glycosylation analysis.

ANG treatment on the experimental mouse model

We used the 0.1% BAK treatment toxicity model twice daily for 1 month to maximize the toxic effect. Two types of ANG (Rh-ANG and ANG-FcK) were used, and 4 μL of ANG (50 μg/mL) was administered to mice twice daily for 1 month. We arranged the combinations of toxic and protective substances into six groups: BAK, Rh-ANG, ANG-FcK, Rh-ANG with BAK, ANG-FcK with BAK, and sham-treated control. In each experimental group, mice were analyzed

158 using three different methods: three underwent ultrastructural analysis, three underwent
159 immunohistochemical analysis, and three underwent microbead injection to analyze the outflow
160 pathway. Mice were treated with ANG 3 days before BAK administration and the two
161 substances were administered at 10-minute intervals.

162 IOP was measured at 6 pm daily without sedation, and mice were euthanized 4 weeks after
163 BAK and/or ANG treatment. Their eyes were then prepared for electron microscopy or
164 immunohistochemistry. Microbeads were injected into three eyes in each experimental group
165 before mice were sacrificed under general anesthesia to evaluate the conventional outflow
166 pathway. The anterior chambers of eyes were cannulated with a 30-gauge needle connected by
167 tubing to a 1-mL syringe filled with green fluorescent beads (100 nm, carboxylate modified
168 FluoSpheres, 1:750 dilution; Molecular Probes, Eugene, OR, USA) and were loaded into a
169 microdialysis infusion pump (World Precision Instruments, Sarasota, FL, USA). 10 μL of liquid
170 was infused into the anterior chamber at 0.167 μL/min for 1 hour. The experimental protocols are
171 summarized in Fig. S1.

172 **Immunohistochemical and ultrastructural analyses**

173 We embedded and froze 36 eyes in Optimal Cutting Temperature Compound (Tissue-Tek, Cat
174 #4583; Sakura Americas, Torrance, CA, USA). Sagittal cryosectioning was performed through
175 the entire anterior–posterior extension of the globe at a thickness of 10-μm. Sections were stored
176 at −80°C and dried for 10 minutes at room temperature. After we washed the sections three times
177 with PBS (Welgene, Gyeongsangbuk-do, Korea) for 10 minutes each, we drew circles along the
178 tissues using a PAP pen (Vector, Burlingame, CA, USA). The sections were fixed with 4%
179 paraformaldehyde (Santa Cruz Biotechnology, Santa Cruz, CA, USA) for 15 minutes, incubated
180 with 0.1% Triton X-100 (Sigma-Aldrich, St. Louis, MO, USA) for 5 minutes for

permeabilization, and washed three times with PBS for 10 minutes each. Slides were incubated in PBS and 1% BSA (Gibco; Thermo Fisher Scientific, Inc.) for 1 hour at room temperature for blocking. Sections were washed once for 10 minutes and incubated with primary antibodies in blocking solution at 4°C overnight. Primary antibodies included collagen type Ⅰ (ab34710, 1:100; Abcam), collagen type Ⅳ (ab6586, 1:100; Abcam), fibronectin (sc-69681, 1:100; Santa Cruz), laminin (ab11575, 1:100; Abcam), and α-smooth muscle actin (α-SMA) (sc-53142, 1:100; Santa Cruz). After being washed three times (10 minutes each), sections were incubated for 1 hour with Cy2 (green) and Cy3 (red) secondary antibodies (1:250; Jackson ImmunoResearch, West Grove, PA, USA). Sections were washed, counter-stained with Hoechst 33258 (1:1000), and mounted with a drop of AquaPolyMount (Polysciences, Warrington, PA, USA). We obtained images using the fluorescence microscope, Imager D2 (Zeiss, Oberkochen, Germany).

For ultramicroscopy, we fixed 18 eyes overnight in cold 2.5% glutaraldehyde, then in 1 osmium tetroxide for 1 hour. After dehydration in a graded acetone series, tissues were embedded in Epon resin, and 0.5-µm semithin or 70-nm ultrathin sections were cut using an ultramicrotome. Semithin sections were stained with toluidine blue. Ultrathin sections were placed on 200-mesh copper grids and double stained with 4% uranyl acetate for 20 minutes and 0.2% lead citrate for 5 minutes. To obtain tangential sections parallel to the plane of the inner wall, we took consecutive semithin sections through the cornea and sclera in a plane parallel to the limbus's outer surface. Once we reached the lumen of Schlemm's canal (SC), we removed consecutive ultrathin sections until we reached the inner wall of SC, juxtacanalicular connective tissue (JCT), and the lamellated TM. Semithin sections were viewed using an Olympus CX22 microscope (Tokyo, Japan), and ultrathin sections were viewed using an electron microscope (HT7700; Hitachi High-Tech Science Corp., Tokyo, Japan) at 80 kV.

204

205 **Statistical analysis**

206 Our results are expressed as means ± standard errors, and normality and equal variances in
207 groups were tested. Analysis of variance (ANOVA) was used to analyze IOP differences across
208 three or more groups at each timepoint, and repeated measures ANOVA was used to compare the
209 baseline IOP during the follow-up period. We included Tukey's tests, Bonferroni's methods,
210 Duncan's tests, and Dunnett's T3 tests in post-hoc analyses. The probability level for statistical
211 significance was set at 5%. Data were recorded and analyzed using SPSS for Windows, version
212 18.0 (SPSS Inc., Chicago, IL, USA).

Results

BAK effect on intraocular pressure

The mean IOP changes in response to various BAK concentrations are shown in Fig. 1A. After 2 weeks of treatment twice a day, 0.1% and 0.2% BAK increased the mean IOP. The IOP was higher in these groups than in the sham-operated control group over the 16-week period, although treatment was performed for 4 weeks. At 4 weeks, 0.1% BAK treatment significantly induced an increase in IOP by approximately 36% (17.3 ± 1.0 mmHg) compared to that of the control group (12.7 ± 0.6 mmHg, $P < 0.01$). This group's IOP remained higher at 6 weeks (23.8 ± 1.2 mmHg) and 12 weeks (24.6 ± 2.3 mmHg) than the control group at the same points in time (14.8 ± 3.0 mmHg and 16.1 ± 5.1 mmHg, $P < 0.01$).

The mean IOP was significantly higher in the 0.2% BAK group than in the control group at 4 weeks (16.5 ± 2.4 mmHg, $P = 0.02$) and at 6 weeks (21.1 ± 1.3 mmHg, $P < 0.01$). The IOP under 0.01% and 0.02% BAK treatments and subconjunctival 0.1% BAK injection was not significantly different from that of the control group, except for 0.02% BAK at 1 week (10.3 ± 1.3 mmHg vs. 14.9 ± 1.6 mmHg in the control group; $P = 0.03$). In the toxic BAK-induced TM degeneration group, we administered a 0.1% BAK treatment twice a day for 4 weeks.

Expression and purification of ANG-FcK in transgenic plants

We examined ANG-FcK expression in randomly selected transgenic plants using western blotting (Fig. 2A). The Rh-ANG protein band was detected at approximately 15 kDa and ANG-FcK was detected at approximately 44 kDa. No band was observed in the non-transgenic plant. We purified ANG-FcK from leaves harvested from transgenic tobacco plants. Protein A column

purification yielded an average of 2 mg of plant-derived ANG-FcK per kg of fresh leaves from a line with high protein expression. SDS-PAGE analysis of purified ANG-FcK revealed one major band (44 kDa, Fig. 2B).

Effect of ANG on BAK-induced changes in intraocular pressure

The mean IOP after 0.1% BAK treatment continued to increase and was significantly higher than that of the other groups at 3 weeks (15.2 ± 2.1 mmHg, $P < 0.01$) and 4 weeks (15.7 ± 1.7 mmHg, $P < 0.01$) (Fig. 2C and 2D). There were few IOP differences between the single Rh-ANG or ANG-FcK treatments and the control group, and inter- and intra-group variability was low (Fig. 2E). For treatments with Rh-ANG or ANG-FcK with BAK, the mean IOP was similar to those of single Rh-ANG and ANG-FcK treatments and the control group at 3 weeks. However at 4 weeks, Rh-ANG with BAK was elevated to 12.1 ± 1.8 mmHg ($P < 0.01$) and ANG-FcK with BAK to 11.6 ± 0.4 mmHg ($P < 0.05$), although these values were lower for the single BAK group ($P < 0.01$) (Fig. 2C, 2ED and 2E).

Immunohistochemical analysis of the effects of ANG on BAK response

We observed that type I collagen's Cy3 labeling in the outflow tissue along the iridocorneal angle was more pronounced in BAK-treated eyes than in the single ANG and control groups (Fig. 3A). The type Ⅰ collagen labeling in the TM region adjacent to the corneal endothelium was patchy and thin in the control (Fig. 3A) and single Rh-ANG (Fig. 3B) and ANG-FcK (Fig. 3C) groups. However, we observed more intense and broader labeling in the single BAK (Fig. 3D) and Rh-ANG with BAK (Fig. 3E) and ANG-FcK with BAK (Fig. 3F) groups. This labeling pattern was similar across type Ⅳ collagen (Fig. 3G to 3L) and fibronectin (Fig. 3M to 3R).

259 Type Ⅳ collagen and fibronectin labeling was more prominent in BAK-treated eyes (especially
260 those in the single BAK-treated group) than in the single ANG and control groups. The positive
261 laminin labeling was more noticeable in the single BAK-treated group (Fig. 4 D) than in the Rh-
262 ANG with BAK (Fig. 4E) and ANG-FcK with BAK (Fig. 4F) groups, but was barely detectable
263 in the single ANG and control groups (Fig. 4A to 4C). We only detected spotty positive α-SMA
264 labeling in the inner sclera of the TM layers adjacent to SC in the single BAK-treated group (Fig.
265 4J), not in any ANG-treated and control groups. In the ciliary body, type Ⅰ, Ⅳ collagen, and
266 fibronectin labeling was observed in the epithelium, and laminin and α-SMA labeling was more
267 apparent in the stroma layer (Fig. 3 and 4).
268 Fluorescent bead deposition traces the flow of aqueous humor, and its intensity is correlated
269 with TM outflow function (Li et al., 2016; Swaminathan et al., 2013). Green fluorescent beads
270 were present in all of the experimental groups' outflow tissues, but deposition intensity
271 decreased in the single BAK-treated group (Fig. 4P). The sparsely deposited fluorescent beads
272 suggest an abnormal TM outflow function resulting from BAK treatment. The cumulative bead
273 distribution data from the single BAK-treated group can be found in Fig. S2. The Rh-ANG and
274 ANG-FcK with BAK groups exhibited more prominent deposition of green fluorescent beads in
275 their outflow tissues, but these results were based on a qualitative analysis.
276
277 **TM histological and ultrastructural changes**
278 After BAK treatment, the characteristic structure of outflow tissues showed little difference
279 under a light microscope (Fig. 1B to 1E). Based on our observations of the ultrathin sections,
280 BAK treatment led to a thickening of the lamina beam in the TM. In particular, we observed
281 hyperthrophied JCT and the accumulation of fibrillar material within the JCT underlying the

SC's inner wall. These were prominent when compared with the empty spaces within the control group's JCT (Fig. 5A and 5B). An increased density and multidirectional array of fibrillar material were also seen in the single BAK-treated group (Fig. 5C and 5D), similar to the "fingerprint"-like basement membrane described in human eyes treated with corticosteroids (Johnson et al. 1997).

There were no remarkable differences between the TM ultrastructures of the Rh-ANG with BAK group (Fig. 5E and 5F) and the ANG-FcK with BAK group (Fig. 5G and 5 H). These groups showed some similarities such as a thickness of lamina beam and empty spaces within the JCT. The fibrillar material was denser than that of the control group, but sparser than that of the single BAK-treated group. Although we did not do a quantitative analysis, we found more intracellular organelles in the ANG and BAK-treated groups than in the control group.

294 **Discussion**

295 In this study, we examined the toxicity of chronic BAK exposure on the TM and ANG's
296 defenses against changes in the trabecular outflow pathway. We induced the structural and
297 functional degeneration of the TM through BAK treatment in a mouse model. Co-treatment with
298 ANG successfully preserved the outflow function of the TM, suggesting that ANG prevents
299 fibrosis.

300 Additionally, we developed ANG-FcK, which has important practical applications. The
301 greater molecular weight of ANG-FcK (44 kDa) over Rh-ANG (15 kDa) enhanced protein
302 stability, facilitated purification, and improved yield. ANG-FcK was similar to Rh-ANG with
303 respect to IOP, flow of aqueous humor, and ultrastructural changes in the BAK-induced TM
304 degenerative mouse model. Purifying plant-derived ANG-FcK yielded an average of 2 mg per kg
305 of fresh leaves. With a cost of approximately U.S. 1,000 dollars per 250 μg of Rh-ANG, 1 kg of
306 transgenic plants is worth approximately U.S. 8,000 dollars of conventional protein. To the best
307 of our knowledge, this is the first study to apply molecular farming techniques in ophthalmology,
308 and our production of recombinant ANG may be beneficial to this field.

309 Although BAK is the most common preservative used in ophthalmic solutions, its effects on
310 IOP or outflow in vivo have not been explored (Rasmussen et al. 2014). After 0.1% and 0.2%
311 BAK topical drops delivered twice a day for 4 weeks in our mouse model, the IOP rose
312 significantly at 4 weeks and remained elevated for 2 additional weeks. This was higher than the
313 IOP for other concentrations and the 0.1% BAK subconjunctival injection. These findings differ
314 from the results of Baudouin et al. (2012) who found that IOP significantly increased 7 days after
315 100 μL of 0.01% BAK subconjunctival injection and remained high for 6 additional days after a
316 second injection on day 7. A major reason for these differences could be the animal model used.

Baudouin et al. (2012) injected 100 μL of BAK into the subconjunctival space of rats weighing 300 to 350 g. In our study, we performed a single injection of 10 μL into the subconjunctival space of mice weighing 21 to 24 g. This might explain the lack of a significant change in IOP despite a higher BAK concentration. In a mouse model, it is difficult to inject 10 μL into the subconjunctival space without any losses. Moreover, the administration of topical drops is more suitable for a chronic exposure model.

The IOP of the combination of ANG and BAK was lower than that the IOP of BAK alone, but was greater than that of eyes not exposed to BAK at 4 weeks. Our results are in agreement with the findings of an earlier experimental study (Kim et al., 2016) where ANG lowered IOP in both normal and elevated rat models using the vortex vein cauterization method. ANG also conserved the conventional outflow of aqueous humor via the TM after BAK treatment. Fluorescent beads were deposited along the outflow tract in the ANG and control groups, but were sparse in the BAK-induced toxicity model. The cumulative distribution of microbeads was sparse across the parallel sections of all three single BAK-treated mouse models (Fig. S2). Although it was based on a subjective analysis since there are low and high-flow regions in the 360-degree circumference of the TM, these results indicate that BAK creates an abnormal outflow of aqueous humor, which is consistent with previous results (Swaminathan et al., 2013; Zhang et al., 2009). Cross-sectional images cannot represent the whole TM, but analyses of fluorescence intensities on flat-mounted sections have been suggested as helpful for this task.

Both the lamina thickness and fibrillar material density increased, and we observed type Ⅰ, type Ⅳ collagen, fibronectin, laminin, and α-SMA fibrogenic markers (Faralli et al., 2019; Ko & Tan, 2013; Pattabiraman et al., 2014) in the BAK-induced toxicity model. BAK caused an epithelial mesenchymal transition-like phenomenon and myofibroblast-like phenotypic changes

in the TM. These changes caused TM cells to abundantly express fibronectin, activate motility, and switch to a myofibroblast-like phenotype, simultaneously strengthening the actin cytoskeleton and extracellular matrix. Fibronectin regulates the deposition of collagen Ⅳ and laminin (Faralli et al., 2019). Overall, these changes cause an increase in TM resistance to aqueous humor outflow (Takahashi et al., 2014; Tamm, 2013). In eyes co-treated with ANG and BAK, we did not detect α-SMA, and the overall ultrastructural configuration was similar to that of the control. However, the fibrillar material density had increased and extracellular matrix markers such as collagen Ⅳ, fibronectin, and laminin were more abundant than in the single ANG and control groups. These findings confirm that ANG defends against fibrosis and myofibroblast-like phenotypic changes induced by BAK by maintaining the proper ultrastructure for aqueous humor outflow.

Our study has its limitations. First, the BAK concentration we used was higher than those used in commercial eye drops. However, we used BAK that had accumulated in the TM, iris, and lens samples during cataract and glaucoma surgery in patients after long-term administration of BAK-containing medication (Desbenoit et al., 2013). Second, the immunohistochemical and ultrastructural findings in our study were based on subjective analyses. Quantifiable methods such as measuring effective filtration areas on anterior segment images (Li et al., 2016; Swaminathan et al., 2013) and ultrastructural analysis of basement membrane material length (Overby et al., 2014) are needed for more comprehensive data. Third, extra in vitro experimental studies are necessary to investigate the protective mechanism of ANG against BAK. Previous studies showed that ANG may activate Akt-mediated signals for nitric oxide production and TM remodeling by regulating matrix metalloproteinase and rho-kinase (Kim et al., 2016). Finally, further research on ANG's effect on retinal ganglion cells may clarify its function and improve

its clinical effectiveness. Because glaucoma is an ocular neurodegenerative disease characterized by the progressive death of retinal ganglion cells, the importance of ANG enrichment in normal motor neurons has been observed in studies on amyotrophic lateral sclerosis, a fetal neurodegenerative disease (Kieran et al., 2008).

Conclusions

In conclusion, ANG's protective effect on TM may involve an anti-fibrotic function with a less extensive ultrastructural change that retains outflow function than exposure to single toxic substance such as BAK. Plant-derived ANG-FcK's protective effect is similar to that of Rh-ANG, and it is a promising candidate for an alternative eye drop additive. Future studies should focus on ANG's detailed defense mechanism and potential applications in glaucoma management.

Acknowledgements

The authors wish to thank medical laboratory technologist Dae Young Kim, Department of Pathology, Konyang University Hospital, Daejeon, Korea, for their electron microscopy technical support.

References

Baudouin C. 2008. Detrimental effect of preservatives in eyedrops: implications for the treatment of glaucoma. *Acta Ophthalmol* 86:716-726. 10.1111/j.1755-3768.2008.01250.x

Baudouin C, Denoyer A, Desbenoit N, Hamm G, and Grise A. 2012. In vitro and in vivo experimental studies on trabecular meshwork degeneration induced by benzalkonium chloride (an American Ophthalmological Society thesis). *Trans Am Ophthalmol Soc* 110:40-63.

Brignole-Baudouin F, Desbenoit N, Hamm G, Liang H, Both JP, Brunelle A, Fournier I, Guerineau V, Legouffe R, Stauber J, Touboul D, Wisztorski M, Salzet M, Laprevote O, and Baudouin C. 2012. A new safety concern for glaucoma treatment demonstrated by mass spectrometry imaging of benzalkonium chloride distribution in the eye, an experimental study in rabbits. *PLoS One* 7:e50180. 10.1371/journal.pone.0050180

Chang C, Zhang AQ, Kagan DB, Liu H, and Hutnik CM. 2015. Mechanisms of benzalkonium chloride toxicity in a human trabecular meshwork cell line and the protective role of preservative-free tafluprost. *Clin Exp Ophthalmol* 43:164-172. 10.1111/ceo.12390

Desbenoit N, Schmitz-Afonso I, Baudouin C, Laprevote O, Touboul D, Brignole-Baudouin F, and Brunelle A. 2013. Localisation and quantification of benzalkonium chloride in eye tissue by TOF-SIMS imaging and liquid chromatography mass spectrometry. *Anal Bioanal Chem* 405:4039-4049. 10.1007/s00216-013-6811-7

Faralli JA, Filla MS, and Peters DM. 2019. Role of Fibronectin in Primary Open Angle Glaucoma. *Cells* 8. 10.3390/cells8121518

Gao X, and Xu Z. 2008. Mechanisms of action of angiogenin. *Acta Biochim Biophys Sin (Shanghai)* 40:619-624.

Inoue K. 2014. Managing adverse effects of glaucoma medications. *Clin Ophthalmol* 8:903-913. 10.2147/OPTH.S44708

Jamal A, Ko K, Kim HS, Choo YK, Joung H, and Ko K. 2009. Role of genetic factors and environmental conditions in recombinant protein production for molecular farming. *Biotechnol Adv* 27:914-923. 10.1016/j.biotechadv.2009.07.004

Johnson D, Gottanka J, Flugel C, Hoffmann F, Futa R, and Lutjen-Drecoll E. 1997. Ultrastructural changes in the trabecular meshwork of human eyes treated with corticosteroids. *Arch Ophthalmol* 115:375-383.

Kieran D, Sebastia J, Greenway MJ, King MA, Connaughton D, Concannon CG, Fenner B, Hardiman O, and Prehn JH. 2008. Control of motoneuron survival by angiogenin. *J Neurosci* 28:14056-14061. 10.1523/JNEUROSCI.3399-08.2008

Kim KW, Park SH, Oh DH, Lee SH, Lim KS, Joo K, Chun YS, Chang SI, Min KM, and Kim JC. 2016. Ribonuclease 5 coordinates signals for the regulation of intraocular pressure and inhibits neural apoptosis as a novel multi-functional anti-glaucomatous strategy. *Biochim Biophys Acta* 1862:145-154. 10.1016/j.bbadis.2015.11.005

Ko MK, and Tan JC. 2013. Contractile markers distinguish structures of the mouse aqueous drainage tract. *Mol Vis* 19:2561-2570.

Li G, Mukherjee D, Navarro I, Ashpole NE, Sherwood JM, Chang J, Overby DR, Yuan F, Gonzalez P, Kopczynski CC, Farsiu S, and Stamer WD. 2016. Visualization of conventional outflow tissue responses to netarsudil in living mouse eyes. *Eur J Pharmacol* 787:20-31. 10.1016/j.ejphar.2016.04.002

Li S, Yu W, and Hu GF. 2012. Angiogenin inhibits nuclear translocation of apoptosis inducing factor in a Bcl-2-dependent manner. *J Cell Physiol* 227:1639-1644. 10.1002/jcp.22881

427 Lim CY, Lee KJ, Oh DB, and Ko K. 2014. Effect of the developmental stage and tissue position
428 on the expression and glycosylation of recombinant glycoprotein GA733-FcK in
429 transgenic plants. *Front Plant Sci* 5:778. 10.3389/fpls.2014.00778
430 Noecker R, and Miller KV. 2011. Benzalkonium chloride in glaucoma medications. *Ocul Surf*
431 9:159-162.
432 Overby DR, Bertrand J, Tektas OY, Boussommier-Calleja A, Schicht M, Ethier CR, Woodward
433 DF, Stamer WD, and Lutjen-Drecoll E. 2014. Ultrastructural changes associated with
434 dexamethasone-induced ocular hypertension in mice. *Invest Ophthalmol Vis Sci* 55:4922-
435 4933. 10.1167/iovs.14-14429
436 Pattabiraman PP, Maddala R, and Rao PV. 2014. Regulation of plasticity and fibrogenic activity
437 of trabecular meshwork cells by Rho GTPase signaling. *J Cell Physiol* 229:927-942.
438 10.1002/jcp.24524
439 Rasmussen CA, Kaufman PL, and Kiland JA. 2014. Benzalkonium chloride and glaucoma. *J*
440 *Ocul Pharmacol Ther* 30:163-169. 10.1089/jop.2013.0174
441 Rosin LM, and Bell NP. 2013. Preservative toxicity in glaucoma medication: clinical evaluation
442 of benzalkonium chloride-free 0.5% timolol eye drops. *Clin Ophthalmol* 7:2131-2135.
443 10.2147/OPTH.S41358
444 Sack RA, Conradi L, Krumholz D, Beaton A, Sathe S, and Morris C. 2005. Membrane array
445 characterization of 80 chemokines, cytokines, and growth factors in open- and closed-eye
446 tears: angiogenin and other defense system constituents. *Invest Ophthalmol Vis Sci*
447 46:1228-1238. 10.1167/iovs.04-0760
448 Steidinger TU, Standaert DG, and Yacoubian TA. 2011. A neuroprotective role for angiogenin in
449 models of Parkinson's disease. *J Neurochem* 116:334-341. 10.1111/j.1471-

4159.2010.07112.x

Swaminathan SS, Oh DJ, Kang MH, Ren R, Jin R, Gong H, and Rhee DJ. 2013. Secreted protein acidic and rich in cysteine (SPARC)-null mice exhibit more uniform outflow. *Invest Ophthalmol Vis Sci* 54:2035-2047. 10.1167/iovs.12-10950

Takahashi E, Inoue T, Fujimoto T, Kojima S, and Tanihara H. 2014. Epithelial mesenchymal transition-like phenomenon in trabecular meshwork cells. *Exp Eye Res* 118:72-79. 10.1016/j.exer.2013.11.014

Tamm ER. 2013. [Functional morphology of the outflow pathways of aqueous humor and their changes in open angle glaucoma]. *Ophthalmologe* 110:1026-1035. 10.1007/s00347-012-2670-4

Tello-Montoliu A, Patel JV, and Lip GY. 2006. Angiogenin: a review of the pathophysiology and potential clinical applications. *J Thromb Haemost* 4:1864-1874. 10.1111/j.1538-7836.2006.01995.x

Van Buskirk EM, and Cioffi GA. 1992. Glaucomatous optic neuropathy. *Am J Ophthalmol* 113:447-452.

Zhang Y, Toris CB, Liu Y, Ye W, and Gong H. 2009. Morphological and hydrodynamic correlates in monkey eyes with laser induced glaucoma. *Exp Eye Res* 89:748-756. 10.1016/j.exer.2009.06.015

Figure 1

Changes in intraocular pressure (IOP) in response to BAK in mouse models and representative histological stains of the mouse eye TM

(A) The mean IOP increased significantly in response to the instillation of 0.1% and 0.2% BAK at 4 weeks, and remained higher than that of the control group at 6 weeks, although the instillation was maintained for 4 weeks. Error bars represent standard errors of the mean. *P < 0.05 and **P < 0.01 (compared to the control group). (B) Hematoxylin and eosin (H-E) stain of the mouse eye TM under a light microscope. (C) H-E stain of the characteristic architecture of outflow tissues showed little difference by BAK. (D) Masson trichrome (M-T) stain of the mouse eye TM under a light microscope. (E) M-T stain of the characteristic architecture of outflow tissues showed little difference 16 weeks after BAK administration.

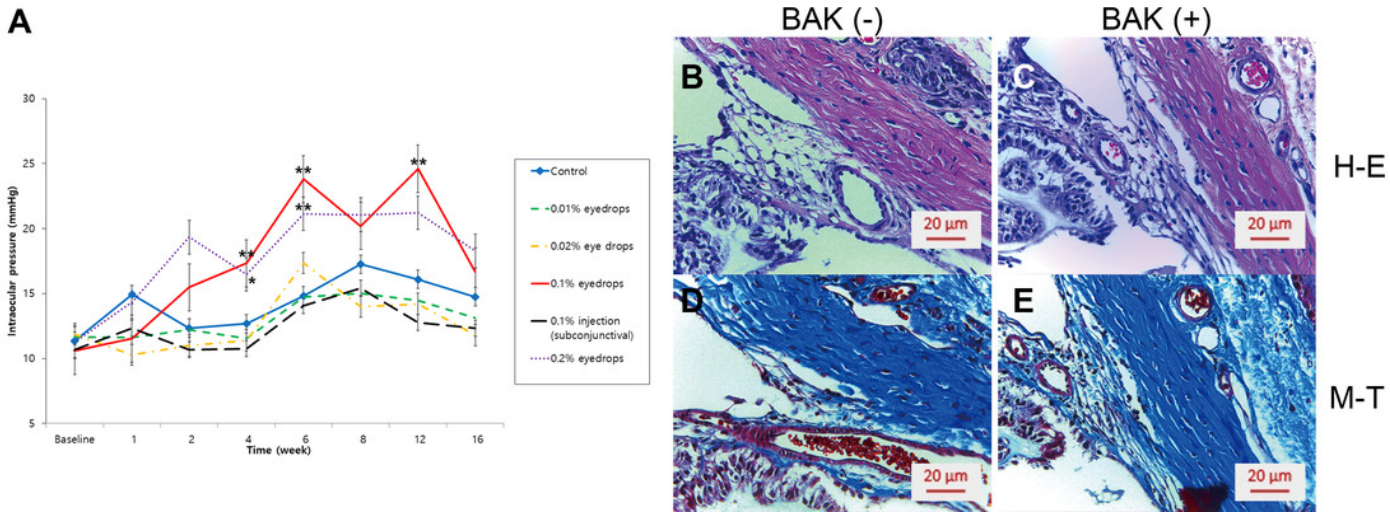

Figure 2

Development of ANG-FcK, and changes in the effects of BAK on intraocular pressure (IOP) in response to ANG

(A) Expression of ANG-FcK in randomly selected transgenic plants. (+), positive control, Rh-ANG; (-), non-transgenic tobacco plant leaf extract. #1167–1187, transgenic plant line number. (B) SDS-PAGE results for purified ANG-FcK. #1–2, purified protein fraction number; Column through: plant extracts passed through a column. (C) The single BAK treatment induced the greatest elevation in mean IOP after 3 weeks among all groups. Cotreatment with Rh-ANG and BAK maintained the initial mean IOP over 3 weeks; however, IOP was elevated at 4 weeks, although it was lower than that for the single BAK treatment group. (D) The change in mean IOP for co-treatment with ANG-FcK and BAK was similar to that for Rh-ANG. IOP was higher than that in the control group, but lower than that in the single BAK treatment group at 4 weeks. (E) There was no significant difference in mean IOP between Rh-ANG and ANG-FcK for the combined use with BAK. Error bars represent standard errors of the mean. *$P < 0.05$ and **$P < 0.01$

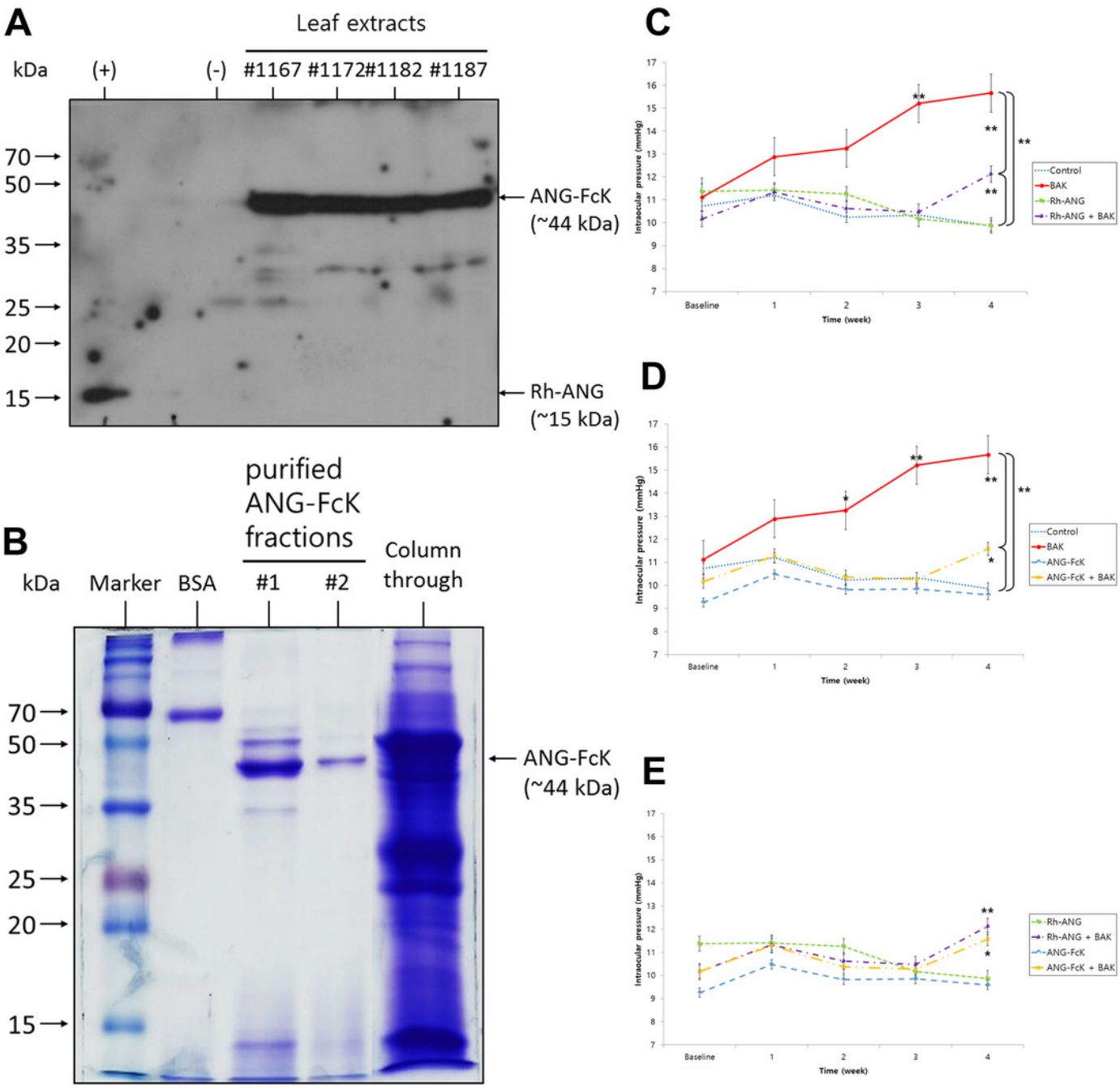
A
Leaf extracts
kDa
(+)
(-)
#1167 #1172#1182 #1187
70
50
35
25
20
15
ANG-FcK
(~44 kDa)
Rh-ANG
(~15 kDa)
B
purified
ANG-FcK
fractions
kDa
Marker
BSA
#1
#2
Column
through
70
50
35
25
20
15
ANG-FcK
(~44 kDa)
C
Intraocular pressure (mmHg)
Time (week)
Baseline
Control
BAK
Rh-ANG
Rh-ANG + BAK
D
Intraocular pressure (mmHg)
Time (week)
Baseline
Control
BAK
ANG-FcK
ANG-FcK + BAK
E
Intraocular pressure (mmHg)
Time (week)
Baseline
Rh-ANG
Rh-ANG + BAK
ANG-FcK
ANG-FcK + BAK

Figure 3

Immunohistochemical labeling of aqueous outflow tissues in a mouse model 01

(A) Sham-treated control. (B) Single Rh-ANG treatment. (C) Single ANG-FcK treatment. (D) Single BAK treatment. (E) Rh-ANG with BAK treatment. (F) ANG-FcK with BAK treatment group. Staining type I collagen (*red*) was present in outflow tissues (*dotted oval*) of the TM and the inner and outer walls of Schlemm's canal in sham-treated control and ANG-treated mice, but the distribution tended to be patchy and thin. BAK-treated mice, in contrast, showed more intense and broader labeling in inner walls of Schlemm's canal (*arrows*). Nuclei were counter-stained with Hoechst (*blue*). (G) Sham-treated control. (H) Single Rh-ANG treatment. (I) Single ANG-FcK treatment. (J) Single BAK treatment. (K) Rh-ANG with BAK treatment. (L) ANG-FcK with BAK treatment group. Staining of type IV collagen (*green*) was more prominent in BAK-treated mice (*arrows*) and especially in eyes of the single BAK-treated group than in single ANG and sham-treated control groups. (M) Sham-treated control. (N) Single Rh-ANG treatment. (O) Single ANG-FcK treatment. (P) Single BAK treatment. (Q) Rh-ANG with BAK treatment. (R) ANG-FcK with BAK treatment group. Staining of Fibronectin (*red*) was more prominent in BAK-treated mice (*arrows*) and especially in eyes of the single BAK-treated group than in single ANG and sham-treated control groups. All images were magnified 200 times. Veh = vehicle for sham-treated control

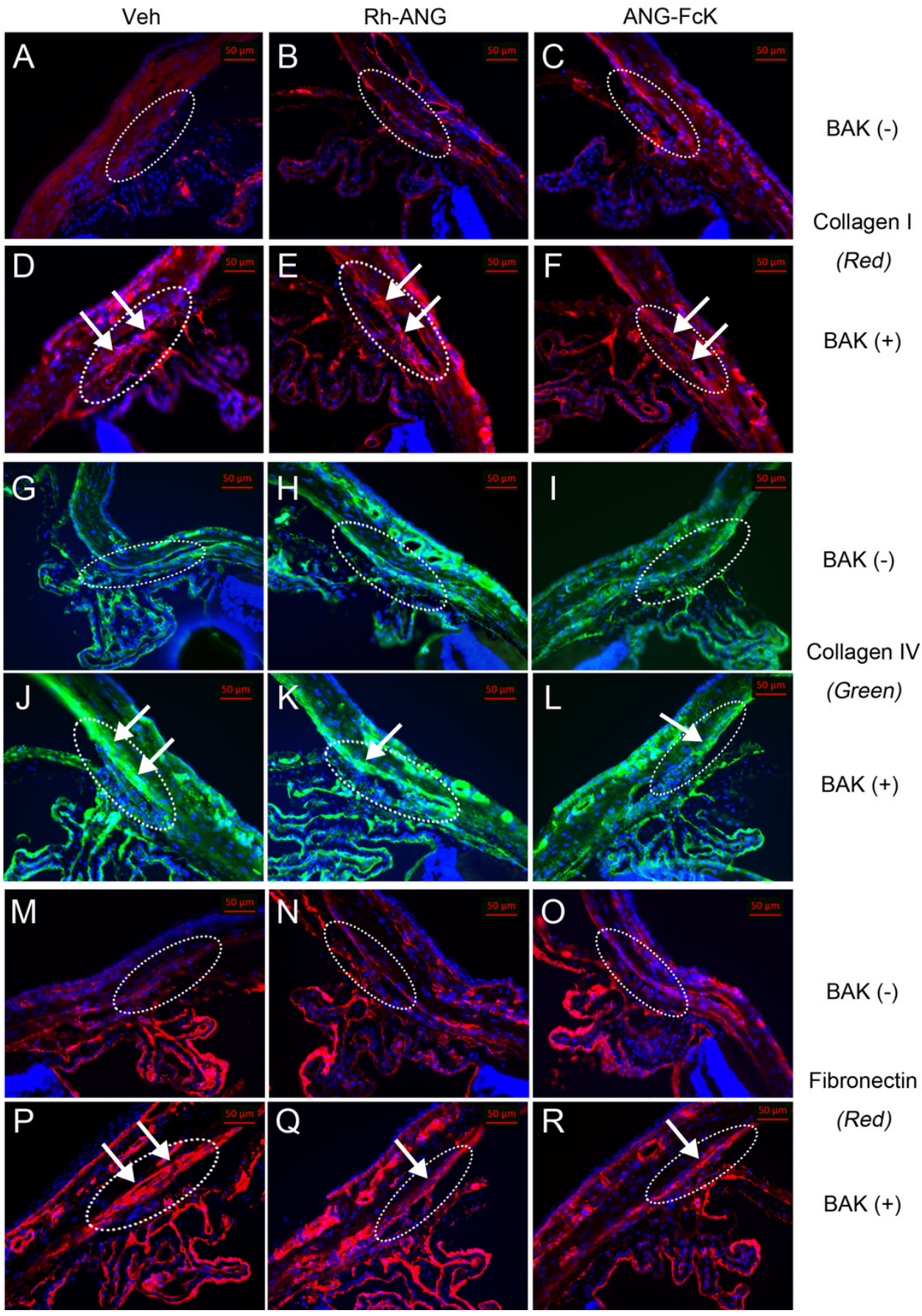
Veh
Rh-ANG
ANG-FcK
A
B
C
D
E
F
G
H
I
J
K
L
M
N
O
P
Q
R
50 µm
BAK (-)
Collagen I
(Red)
BAK (+)
BAK (-)
Collagen IV
(Green)
BAK (+)
BAK (-)
Fibronectin
(Red)
BAK (+)

Figure 4

Immunohistochemical labeling of aqueous outflow tissues in a mouse model 02

(A) Sham-treated control. (B) Single Rh-ANG treatment. (C) Single ANG-FcK treatment. (D) Single BAK treatment. (E) Rh-ANG with BAK treatment. (F) ANG-FcK with BAK treatment group. Staining of laminin (*green*) in the single BAK-treated group was more pronounced in outflow tissues (*dotted oval*) of the TM and the inner and outer walls of Schlemm's canal than in the Rh-ANG or ANG-FcK with BAK groups (*arrowheads*) but it was barely detectable in single ANG and control groups. (G) Sham-treated control. (H) Single Rh-ANG treatment. (I) Single ANG-FcK treatment. (J) Single BAK treatment. (K) Rh-ANG with BAK treatment. (L) ANG-FcK with BAK treatment group. Spotty positive α-SMA labeling (*green*) in the TM layers adjacent to Schlemm's canal (*arrowheads*) was only detected in the eye of the single BAK-treated group, but not in any ANG-treated and control groups. (M) Sham-treated control. (N) Single Rh-ANG treatment. (O) Single ANG-FcK treatment. (P) Single BAK treatment. (Q) Rh-ANG with BAK treatment. (R) ANG-FcK with BAK treatment group. Green fluorescent beads were deposited in outflow tissues; however, they were sparse in the single BAK-treated group. Type I collagen was used for counter-staining (*red*). All images were magnified 200 times. Veh = vehicle for sham-treated control

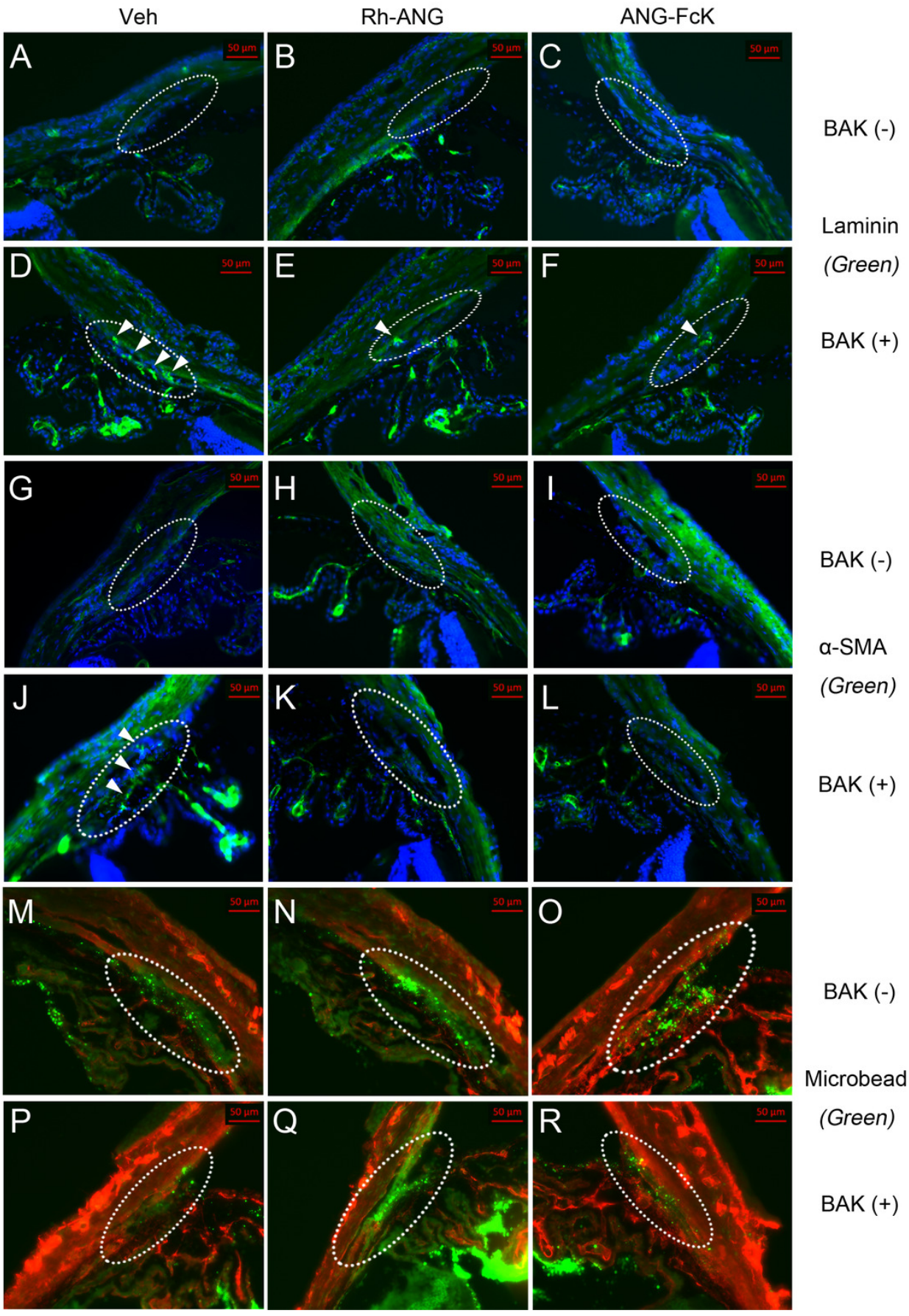
Veh
Rh-ANG
ANG-FcK
A
B
C
D
E
F
G
H
I
J
K
L
M
N
O
P
Q
R
50 μm
BAK (-)
Laminin
(Green)
BAK (+)
BAK (-)
α-SMA
(Green)
BAK (+)
BAK (-)
Microbead
(Green)
BAK (+)

Figure 5

Ultrastructural changes in the TM of mice treated with the combination of BAK and ANG for 4 weeks

Photographs with magnification power of 1,500 were in top row, and those with magnification power of 4,000 were in bottom row. (A) In sham-treated control mice without BAK, optically open spaces (*asterisks*) were often observed between juxtacanalicular connective tissue (JCT) cells. (B) Accumulation of fibrillar material within JCT was sparse and unidirectional (*arrowheads*). (C) In BAK-treated mice, the thickness of the lamina beam increased within the JCT (*arrows*). (D) The JCT was often filled with fine fibrillary material that showed an increased density and multidirectional array (*empty arrowheads*). Increased intracellular organelles were found in the cytoplasm of trabeculocytes with BAK treatment. (E) The ultrastructures of TM for the combination of Rh-ANG with BAK. The thickness of the lamina beam and the empty spaces within the JCT (*asterisks*) were preserved. (F) Fibrillar materials were denser in the combined treatment group than the control group, but sparser than in the single BAK treatment group (*arrowheads*) (G) The ultrastructures of TM and (H) deposition of fibrillar materials for the combination of ANG-FcK with BAK were similar with those of Rh-ANG with BAK.

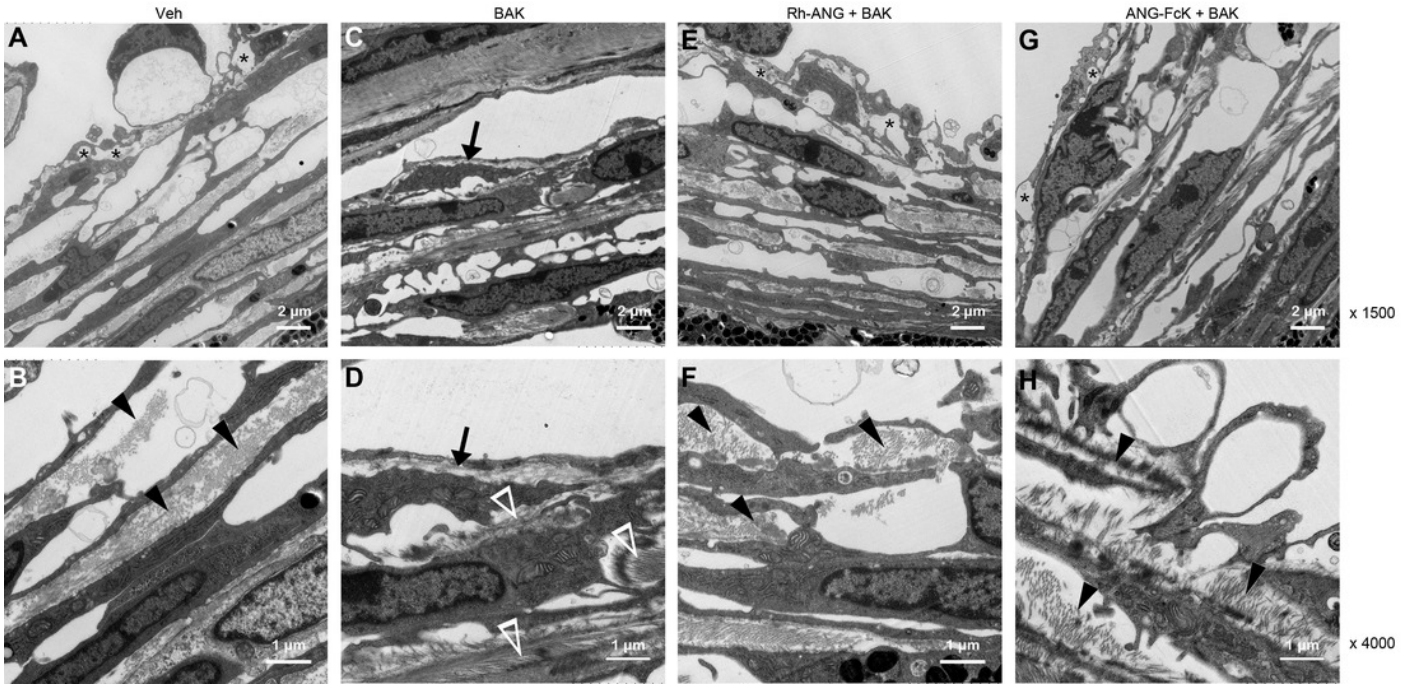
Veh
BAK
Rh-ANG + BAK
ANG-FcK + BAK
A
C
E
G
B
D
F
H
2 µm
1 µm
x 1500
x 4000